$[Ru_3(CO)_9(\mu_3\text{-}S)]^{2-}$ as a Ligand toward $[M(CO)_3(NCCH_3)_3]^+$: Synthesis and Characterization of $HRu_3(CO)_9(\mu_4\text{-}S)M(CO)_3(NCCH_3)_2$ (M = Mn, Re)

Eric J. Voss, Charlotte L. Stern, and Duward F. Shriver*

Department of Chemistry, Northwestern University, Evanston, Illinois 60208-3113

*Received September 22, 1993**

Reactions of the dianionic sulfido cluster $[Ru_3(CO)_9(\mu_3\text{-}S)]^{2-}$ with the lightly stabilized electrophilic cluster-building reagents $[M(CO)_3(NCCH_3)_3]^+$ (M = Mn, Re) produced the mixed-metal sulfido clusters $HRu_3(CO)_9(\mu_4\text{-}S)Mn(CO)_3(NCCH_3)_2$ and $HRu_3(CO)_9(\mu_4\text{-}S)Re(CO)_3(NCCH_3)_2$, which contain a pseudotetrahedral μ_4-sulfido atom. Analogous reactions of $[Ru_3(CO)_9(\mu_3\text{-}S)]^{2-}$ with $[M(CO)_5]^+$ (M = Mn, Re) yielded clusters identified as $HRu_3(CO)_9(\mu_4\text{-}S)Mn(CO)_5$ and $HRu_3(CO)_9(\mu_4\text{-}S)Re(CO)_5$ in solution. The clusters $HRu_3(CO)_9(\mu_4\text{-}S)M(CO)_3(NCCH_3)_2$ (M = Mn, Re) were characterized by liquid secondary ionization mass spectroscopy, and the structure of $HRu_3(CO)_9(\mu_4\text{-}S)Mn(CO)_3(NCCH_3)_2$ was determined by single-crystal X-ray diffraction. These molecules contain the triangular ruthenium metal array capped by an $SM(CO)_3(NCCH_3)_2$ moiety. The μ_4-sulfido ligand may be viewed as a five-electron donor to the ruthenium triangle and a one electron donor to the pendant metal. The hydrogen atom, located in the X-ray experiment, resides on the ruthenium framework. Crystal data for $HRu_3(CO)_9(\mu_4\text{-}S)Mn(CO)_3(NCCH_3)_2$: monoclinic ($P2_1/c$ (No. 14)), a = 16.418(4) Å, b = 8.865(1) Å, c = 17.550(4) Å, β = 96.73(2)°, Z = 4, R (R_w) = 0.038 (0.042).

Introduction

Organometallic cluster compounds[1-3] containing p-block nonmetals have come under increasing investigation because of their interesting structures and reactivity patterns.[4] The main-group heteroatoms in these clusters display a wide variety of bonding modes and stabilize unusual cluster geometries such as "butterfly" arrangements of transition metals.[5] The recent incorporation of oxygen into such clusters[6-8] prompted the present exploration of analogous sulfur-containing clusters.

Although many organometallic metal–sulfide clusters are known, the synthetic reactions are often ill-defined, and complex mixtures of products result.[9,10] The systematic synthetic route chosen here is based on the utilization of the $[Ru_3(CO)_9(\mu_3\text{-}S)]^{2-}$ cluster (**I**) as a ligand toward labile transition-metal carbonyl complexes. This general reaction has been used by Brown, Salter, Hudson, and McPartlin to generate coinage metal[11] complexes of **I** (Scheme 1) and by Schauer and co-workers in the synthesis of the first metal–oxo butterfly complex.[6] The structures observed in these two cases differ from those formed in the present research and the related work of Richter and Vahrenkamp[12] and of Takacs and Marko.[13]

The sulfido ligand is able to adapt a variety of coordination modes including μ, μ_3, and μ_4 (Figure 1).[14] In binuclear systems

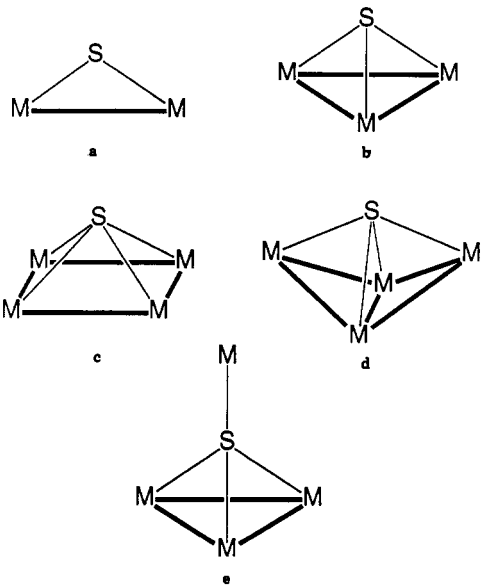

Figure 1. Drawings showing the μ, μ_3, and μ_4 coordination modes of the sulfido ligand.

Scheme 1

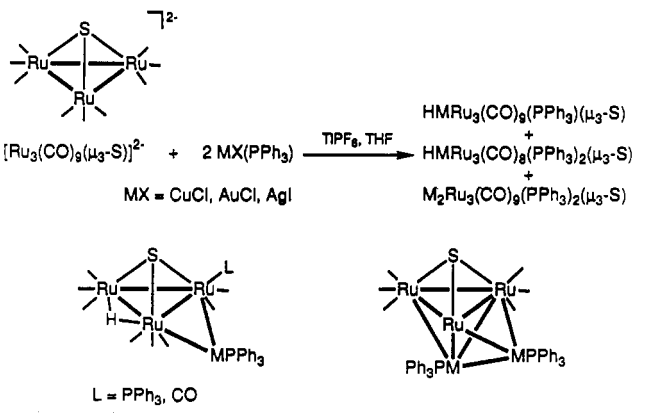

such as the oldest known metal–sulfur complex, red Roussain salt $K_2[(NO)_2Fe(\mu\text{-}S)_2Fe(NO)_2]$, each bridging sulfur atom spans

* Abstract published in *Advance ACS Abstracts*, February 15, 1994.

(1) *Transition Metal Clusters*; Johnson, B. F. G., Ed.; John Wiley and Sons: New York, 1980.
(2) *The Chemistry of Metal Cluster Complexes*; Shriver, D. F., Kaesz, H. D., Adams, R. D., Eds.; VCH Publishers, Inc.: New York, 1990.
(3) Mingos, D. M. P.; Wales, D. J. *Introduction to Cluster Chemistry*; Prentice Hall: Englewood Cliffs, NJ, 1990.
(4) Whitmire, K. H. *J. Coord. Chem. B* **1988**, *17*, 95.
(5) Sappa, E.; Tiripicchio, A.; Carty, A. J.; Toogood, G. E. *Prog. Inorg. Chem.* **1987**, *35*, 437.
(6) Schauer, C. K.; Shriver, D. F. *Angew. Chem., Int. Ed. Engl.* **1987**, *26*, 255.
(7) Schauer, C. K.; Harris, S.; Sabat, M.; Voss, E. J.; Shriver, D. F. Manuscript in preparation.
(8) Voss, E. J.; Sabat, M.; Shriver, D. F. *Inorg. Chem.* **1991**, *30*, 2705.
(9) Adams, R. D.; Tasi, M. *J. Clust. Sci.* **1990**, *1*, 249.
(10) Adams, R. D. *Polyhedron* **1985**, *4*, 2003.
(11) Brown, S. S. D.; Hudson, S.; Salter, I. D.; McPartlin, M. *J. Chem. Soc., Dalton Trans.* **1987**, 1967.
(12) Richter, F.; Vahrenkamp, H. *Angew. Chem., Int. Ed. Engl.* **1978**, *17*, 444.
(13) Takacs, J.; Marko, L. *Transition Met. Chem. (London)* **1985**, *10*, 21.
(14) Vahrenkamp, H. *Angew. Chem., Int. Ed. Engl.* **1975**, 322.

0020-1669/94/1333-1087$04.50/0

a metal–metal bond to form an M_2S triangle[15-17] (Figure 1a). Metal clusters provide the opportunity for three-coordinate sulfur capping a triangular face (Figure 1b), for example in $H_2Fe_3(CO)_9(\mu_3\text{-}S)$.[18] Among four-coordinate modes observed are capping a square face (Figure 1c) as in $Ru_5(CO)_{15}(\mu_4\text{-}S)$,[19] coordination between the wings of a butterfly cluster (Figure 1d) as in $[PPN][Fe_3Mn(CO)_{12}(\mu_4\text{-}S)]$,[7] and pseudotetrahedral coordination to the three metals of a cluster and a fourth pendant metal (Figure 1e) as in $Co_2Fe(CO)_9(\mu_4\text{-}S)Cr(CO)_5$.[12] The compounds reported in this paper contain a similar pseudotetrahedral sulfido ligand.

Experimental Section

General Procedures and Materials. All manipulations were carried out under an atmosphere of prepurified, dry nitrogen using standard Schlenk and syringe techniques.[20] Solids were manipulated in a Vacuum Atmospheres glovebox equipped with a recirculator and Dri-Train system. All solvents were distilled from the appropriate drying agents in an air-free environment prior to use.[21] Bis(triphenylphosphine)nitrogen(1+) chloride ($[PPN]^+Cl^-$) was purchased from Alpha Products and was dried in an oven at 110 °C for 24 h prior to use. H_2S gas (Matheson Gas) was used as received. Florisil (magnesium silicate) 60–100 mesh was purchased from Aldrich Chemicals and was dried in an oven at 110 °C for 24 h prior to use. Potassium hydroxide was finely ground with a mortar and pestle in the drybox. The compounds $Ru_3(CO)_{12}$,[22] $[Mn(CO)_3(NCCH_3)_3][PF_6]$,[23] $[Re(CO)_3(NCCH_3)_3][PF_6]$,[24] $[Mn(CO)_5][OSO_2CF_3]$,[25] and $[Re(CO)_5][OSO_2CF_3]$[25] were prepared by following literature procedures. The compounds $H_2[Ru_3(CO)_9(\mu_3\text{-}S)]$[26] and $[PPN]_2[Ru_3(CO)_9(\mu_3\text{-}S)]$[11] were prepared by using modifications of literature procedures that are described below.

Solution infrared data were collected with CaF_2-windowed cells with 0.1-mm path length, and spectra were recorded on a Bomem MB-100 Fourier transform infrared spectrometer equipped with a DTGS detector. Elemental analyses were performed by Elbach Analytical Laboratories, Postfach 1315, D-5250 Engelskirchen, Germany.

The liquid secondary ion (LSIMS, commonly termed FABMS) mass spectra were obtained on a VG-70SE double-focusing high-resolution mass spectrometer equipped with a VG 11/250J data system. The samples were dissolved in CH_2Cl_2, and 3-nitrobenzyl alcohol (*m*-NBA) was employed as the matrix. Cesium iodide was used as the primary Cs^+ ion source. The primary ion beam (1 μA at 30 kV) impinged on the liquid sample surface. Negative-ion detection was used to collect all mass spectra. The VG software ISO was used to calculate isotopic distributions of molecular ions.

A conventional *R* factor, $R = (\Sigma||I_o| - |I_c||)/\Sigma|I_o|$ (analogous to a crystallographic *R* factor, in which I_o is the observed intensity and I_c is the calculated intensity at a given mass number) was calculated to provide a quantitative measure of the fit between calculated isotopomers of the proposed compound and the observed spectrum. Peaks at least five mass units on either side of the most intense peak in the observed spectrum were used in this calculation. Previous workers[27] have proposed that the mass spectral assignments are satisfactory when the values of *R* are roughly similar to those in acceptable crystal structure determinations. According to this criterion, the mass envelopes are convincingly assigned.

Synthesis of $H_2Ru_3(CO)_9(\mu_3\text{-}S)$. A 300-mL Schlenk flask containing a sample of $Ru_3(CO)_{12}$ (2.00 g, 3.13 mmol) was purged with dry N_2, heptane (60 mL) was added, and the flask was attached to a water-cooled reflux condenser equipped with a nitrogen purge source and a mineral oil bubbler, followed by two OCl^- bleach scrubbers. The entire system was purged with H_2S for 1–2 min, resulting in 1 atm of H_2S over the solution. The system was then isolated from the H_2S source, and the connection to the bubbler outlet was retained while the solution was heated to reflux (98 °C) for 2 h. During reflux, the color changed from bright orange to deep orange to orange-red and finally to red-brown. The solution was cooled with a slow N_2 purge, and some yellow solids precipitated from the brown solution. The IR spectrum of the brown solution at this point confirmed the formation of $H_2Ru_3(CO)_9(\mu_3\text{-}S)$.[28] The solution (and solids) were placed onto a 1 cm × 3 cm Florisil pad under N_2, and the purified product was eluted with pentane (~500 mL). Each portion of the golden yellow solution was transferred to a 30 mL Schlenk flask, reduced in volume, and dried under vacuum to yield a powdery bright yellow solid. Isolated yield: 1.62 g (2.75 mmol, 88%). IR (ν_{CO}, pentane): 2118 (m), 2084 (s), 2062 (vs), 2049 (s), 2019 (vs), 2011 (s), 2000 (w), 1996 (w, sh), 1969 (vw) cm^{-1}. ^1H NMR (CD_2Cl_2, δ): −18.95 ppm (hydride). The IR and ^1H NMR data match literature values for this compound.[28,29]

Synthesis of $[PPN]_2[Ru_3(CO)_9(\mu_3\text{-}S)]$. A sample of $H_2Ru_3(CO)_9(\mu_3\text{-}S)$ (500 mg, 0.85 mmol) was placed into a 100 mL Schlenk flask and was suspended in EtOH (15 mL). A solution of KOH (200 mg, 3.60 mmol) in EtOH (15 mL) was added dropwise to the stirred solution of the cluster. Over a period of 1 h, the color changed from yellow to deep red. The formation of $K_2Ru_3(CO)_9(\mu_3\text{-}S)$ was indicated by infrared spectroscopy. IR (ν_{CO}, EtOH): 2061 (m), 2030 (vs), 2000 (vs), 1974 (vs), 1929 (m), 1604 (m) cm^{-1}. A solution of [PPN]Cl (2.00 g, 3.48 mmol) in EtOH (20 mL) was added dropwise to the stirred cluster solution, and light brown solids precipitated. The mixture was stirred for 1 h to allow complete metathesis. The brown solids were isolated by filtration and were washed with EtOH (3 × 10 mL). Crude yield: 770 mg (0.463 mmol, 54%). The $[PPN]_2[Ru_3(CO)_9(\mu_3\text{-}S)]$ extracted into Et_2O (4 × 50 mL) was transferred to a separate flask, dried under vacuum to yield yellow solids, and dissolved in CH_2Cl_2 (10 mL). The bright yellow solution was layered with petroleum ether (30 mL), resulting in golden yellow crystals of $[PPN]_2[Ru_3(CO)_9(\mu_3\text{-}S)]$. Isolated yield: 430 mg (0.26 mmol, 30%). IR (ν_{CO}, CH_2Cl_2): 2060 (w), 2030 (vs), 2000 (vs), 1970 (vs), 1921 (m), 1590 (w) ($[PPN]^+$) cm^{-1}. ^1H NMR (CD_2Cl_2, δ): ~7.6 ppm (multiplet, $[PPN]^+$). The IR and ^1H NMR data match literature values for this compound.[11]

Synthesis of $HRu_3(CO)_9(\mu_4\text{-}S)Mn(CO)_3(NCCH_3)_2$. A sample of $[PPN]_2[Ru_3(CO)_9(\mu_3\text{-}S)]$ (82 mg, 0.05 mmol) in a 30-mL Schlenk flask was dissolved in CH_2Cl_2 (5 mL). A solution containing $[Mn(CO)_3(NCCH_3)_2][PF_6]$ (40 mg, 0.10 mmol) in CH_2Cl_2 (10 mL) was added dropwise until the reaction went to completion, as indicated by infrared spectroscopy (7.5 mL, 1.5 equiv). Solvent was removed under vacuum from this green-orange solution to yield a green-orange oil, which was extracted with Et_2O (20 mL), the extract was filtered (leaving behind white $[PPN][PF_6]$), and the flask was evacuated to yield a yellow powder. This crude solid was dissolved in CH_2Cl_2 (2 mL), and the solution was layered with pentane (12 mL). Orange crystals of $HRu_3(CO)_9(\mu_4\text{-}S)Mn(CO)_3(NCCH_3)_2$ were isolated by filtration, washed with pentane (3 × 3 mL), and briefly vacuum-dried. Isolated yield: 40 mg (0.049 mmol, 98%). IR data are given in Table 1. ^1H NMR (CD_2Cl_2): δ 2.32 (CH_3-CN ligands), −18.72 pm (Ru–*H*–Ru). EDAX indicated the presence of S, Mn, and Ru in the crystals. Anal. Calcd (found) for $C_{16}H_7N_2O_{12}SMnRu_3$: C, 23.74 (24.82); H, 0.87 (0.89); N, 3.46 (3.57); S, 3.96 (3.98); Mn, 6.79 (7.19). The elemental composition of $HRu_3(CO)_9(\mu_4\text{-}S)Mn(CO)_3(NCCH_3)_2$ was confirmed by analysis of the distribution of the isotopomers in the FABMS spectrum reported below. Exposure to the atmosphere was minimized, but the solid compound appears to be stable in air for at least a short period of time.

Synthesis of $HRu_3(CO)_9(\mu_4\text{-}S)Re(CO)_3(NCCH_3)_2$. Samples of $[PPN]_2[Ru_3(CO)_9(\mu_3\text{-}S)]$ (60 mg, 0.036 mmol) and $[Re(CO)_3(NCCH_3)_2][PF_6]$ (30 mg, 0.056 mmol, ~1.5 equiv) were dissolved in acetone (5 mL) in a 30 mL Schlenk flask. The solution was stirred, and the reaction was monitored by infrared spectroscopy. After 4 days, reaction was complete. The solvent was removed under vacuum from the light orange solution to yield a green-yellow oil, which was extracted with Et_2O (20 mL), the extract was filtered (leaving behind white $[PPN][PF_6]$), and the flask

(15) Roussain, J. *Ann. Chim. Phys.* **1858**, *52*, 285.
(16) Seel, F. *Z. Anorg. Allg. Chem.* **1942**, *249*, 308.
(17) Thomas, J. T.; Robertson, J. H.; Cox, E. G. *Acta Crystallogr.* **1958**, *11*, 599.
(18) Marko, L.; Takacs, J.; Papp, S.; Marko-Monostory, B. *Inorg. Chim Acta* **1980**, *45*, L189.
(19) Adams, R. D.; Babin, J. E.; Tasi, M. *Organometallics* **1988**, *7*, 503.
(20) Shriver, D. F.; Drezdzon, M. A. *Manipulation of Air-Sensitive Compounds*; Wiley: New York, 1986.
(21) Gordon, A. J.; Ford, R. A. *The Chemist's Companion*; Wiley: New York, 1977.
(22) Bruce, M. I.; Matisons, J. G.; Wallis, R. C.; Patrick, J. M.; Skelton, B. W.; White, A. H. *J. Chem. Soc., Dalton Trans.* **1983**, 2365.
(23) Drew, D.; Darensbourg, D. J.; Darensbourg, M. Y. *Inorg. Chem.* **1975**, *14*, 1579.
(24) Reimann, R. H.; Singleton, E. *J. Organomet. Chem.* **1973**, *59*, C24.
(25) Nitschke, J.; Schmidt, S. P.; Trogler, W. C. *Inorg. Chem.* **1985**, *24*, 1972.
(26) Adams, R. D.; Katahira, D. A. *Organometallics* **1982**, *1*, 53.
(27) Andrews, M. A.; Kirtley, S. W.; Kaesz, H. D. *Inorg. Chem.* **1977**, *16*, 1556.
(28) Deeming, A. J.; Underhill, M. *J. Organomet. Chem.* **1972**, *42*, C60.
(29) Sappa, E.; Gambino, O.; Cetini, G. *J. Organomet. Chem.* **1972**, *35*, 375.

Table 1. Infrared CO Stretching Frequencies of the Pendant Metal Sulfido Clusters[a]

cluster	solvent	ν_{CO}, cm^{-1}
$HRu_3(CO)_9(\mu 4\text{-}S)Mn(CO)_3(NCCH_3)_2$	Et_2O	2076 m, 2061 vw, 2046 vs, 2018 s, 1993 ms, 1981 sh, 1964 sh, 1933 vw
$HRu_3(CO)_9(\mu_4\text{-}S)Re(CO)_3(NCCH_3)_2$	Et_2O	2076 m, 2066 vw, 2046 vs, 2019 s, 1993 ms, 1981 sh, 1943 ms
$HRu_3(CO)_9(\mu_4\text{-}S)Ru(CO)_3(\eta^2\text{-}CH_2CMe_2NCHNHBu^t)$[35]	C_6H_{12}	2135 s, 2098 s, 2073 m, 2049 vs, 2022 vs, 2011 m, 1999 vs, 1984 m, 1961 w, 1943 w
$HRu_3(CO)_9(\mu_4\text{-}S)Mn(CO)_3(NCCH_3)_2$ + CO gas, 2 days	acetone	2138 w, 2113 w, 2074 w, 2051 vs, 2030 s, 2022 sh, 1998 s, 1976 m
$HRu_3(CO)_9(\mu_4\text{-}S)Mn(CO)_5$	Et_2O	2135 w, 2095 w, 2079 w, 2069 m, 2053 vs, 2027 s, 1995 ms, 1977 m
$HRu_3(CO)_9(\mu_4\text{-}S)Re(CO)_5$	Et_2O	2153 w, 2108 w, 2079 w, 2070 m, 2054 vs, 2027 s, 1994 ms, 1958 w

[a] Legend: vs = very strong; s = strong/ ms = medium strong; m = medium; w = weak; vw = very weak; sh = shoulder.

was evacuated to yield a yellow oil. This crude product was dissolved in CH_2Cl_2 (2 mL), and the solution was layered with pentane (5 mL). Orange-brown crystals of $HRu_3(CO)_9(\mu_4\text{-}S)Re(CO)_3(NCCH_3)_2$ were isolated by filtration, washed with pentane (3 × 3 mL), and briefly vacuum-dried. Isolated yield: 20 mg (0.021 mmol, 59%). IR data are given in Table 1. Anal. Calcd (found) for $C_{16}H_7N_2O_{12}SMnRu_3$: C, 20.43 (21.89); H, 0.75 (0.94); N, 2.98 (2.92); S, 3.41 (3.17). The elemental composition of $HRu_3(CO)_9(\mu_4\text{-}S)Re(CO)_3(NCCH_3)_2$ was confirmed by analysis of the distribution of the isotopomers in the FABMS spectrum reported below. Exposure to the atmosphere was minimized, but the solid compound appears to be stable in air for at least a short period of time.

X-ray Crystal Structure Determination of $HRu_3(CO)_9(\mu_4\text{-}S)Mn(CO)_3(NCCH_3)_2$. An orange, platelike crystal of $HRu_3(CO)_9(\mu_4\text{-}S)Mn(CO)_3(NCCH_3)_2$ having approximate dimensions of 0.50 × 0.40 × 0.10 mm was mounted on a glass fiber using high-vacuum grease and immediately put into the cold N_2 stream. All measurements were made on an Enraf-Nonius CAD-4 diffractometer with graphite-monochromated Mo Kα radiation.

Cell constants and an orientation matrix for data collection, obtained from a least-squares refinement using the setting angles of 25 carefully centered reflections in the range $20.02 < 2\theta < 21.82°$, corresponded to a monoclinic cell with dimensions a = 16.418(4) Å, b = 8.865(1) Å, c = 17.550(4) Å, β = 96.73(2)°, and V = 2537(2) Å^3. For Z = 4 and fw 809.45, the calculated density is 2.009 g/cm^3. On the basis of the systematic absences of $h0$ ($l \neq 2n$) and $0k0$ ($k \neq 2n$) and the successful solution and refinement of the structure, the space group is $P2_1/c$ (No. 14).

Data were collected at a temperature of −120 ± 1 °C using the ω–θ scan technique to a maximum 2θ value of 55.0°. ω scans of several intense reflections, made prior to data collection, had an average width at half-height of 0.30° with a takeoff angle of 2.8°. Scans of (1.00 + 0.35 tan θ)° were made at speeds ranging from 3.0 to 16.0°/min (in ω).

Of the 6413 reflections collected, 6208 were unique. The intensities of three representative reflections, measured every 90 min, remained constant throughout data collection, so no decay correction was applied. The linear absorption coefficient for Mo Kα is 23.2 cm^{-1}. An analytical absorption correction was applied with transmission factors ranging from 0.38 to 0.80. The data were corrected for Lorentz and polarization effects. A correction for secondary extinction was applied (coefficient = 0.178 43 × 10^{-6}).

The structure was solved by direct methods using SHELXS-86.[30] The three ruthenium and one manganese atoms were located in the E map and other non-hydrogen atoms were found by difference Fourier techniques. The full-matrix least-squares refinement included anisotropic thermal parameters on all non-hydrogen atoms of the cluster. The hydrogen atoms, other than H1, were fixed in calculated positions and were included in structure factor calculations but were not refined. H1 was located on the difference map but was not refined. The final cycle of full-matrix least-squares refinement[31] was based on 3946 observed reflections ($I > 3.00\sigma(I)$) and 317 variable parameters and converged (largest parameter shift was 0.01 times its esd) with unweighted and weighted agreement (Table 2). The maximum and minimum peaks on the final difference Fourier map corresponded to 1.64 and −1.25 e/Å^3, respectively.

Table 2. Summary of the Crystallographic Data for $HRu_3(CO)_9(\mu_4\text{-}S)Mn(CO)_3(NCCH_3)_2$

empirical formula	$MnRu_3C_{16}H_7N_2O_{12}S$
fw	809.45
space group	$P2_1/c$ (No. 14)
lattice parameters	
a	16.418(4) Å
b	8.865(1) Å
c	17.550(4) Å
β	96.73(2)°
V	2537(2) Å^3
Z value	4
temp	−120 °C
radiation	Mo Kα (λ = 0.710 69 Å)
ρ_{calcd}	2.119 g cm^{-3}
μ(Mo Kα)	23.23 cm^{-1}
transm coeff	0.38–0.80
p factor	0.03
$R(F)$[a]	0.038
$R_w(F)$[b]	0.042

[a] $R(F) = (\sum||F_o|-|F_c||)/\sum|F_o|$. [b] $R_w(F) = [(\sum w(|F_o|-|F_c|)^2)/\sum wF_o^2]^{1/2}$.

Neutral-atom scattering factors were taken from Cromer and Waber.[32] Anomalous dispersion effects were included in F_c.[33] The values for $\Delta f'$ and $\Delta f''$ were those of Cromer.[34] All calculations were performed using the TEXSAN 4.0 crystallographic software package of the Molecular Structure Corp. on a Micro VAX 3600 computer.[35] A summary of the crystallographic data is shown in Table 2.

Results and Discussion

Preparation of the Three-Metal Sulfido-Capped Ruthenium Clusters $H_2Ru_3(CO)_9(\mu_3\text{-}S)$ and $[Ru_3(CO)_9(\mu_3\text{-}S)]^{2-}$. The compound $H_2Ru_3(CO)_9(\mu_3\text{-}S)$ has been prepared by acidification of $HRu_3(CO)_{10}SEt$[36] and by the high-pressure reaction of $Ru_3(CO)_{12}$ with elemental sulfur,[29] but yields were low in both cases. Adams and Katahira[26] reported a high-yield synthesis of $H_2Ru_3(CO)_9(\mu_3\text{-}S)$ in which $Ru_3(CO)_{12}$ was refluxed in heptane under H_2S gas (eq 1). Since the reported synthesis lacks detail, a full

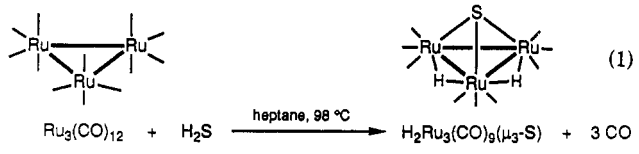

(1)

description of the procedure is presented in the Experimental Section of this paper. The synthesis and purification yielded bright yellow powder obtained in high yield (>80%) which was used without further purification.

(30) Sheldrick, G. M. *SHELXS-86: A Program for Crystal Structure Determination*; University of Goettingen: Goettingen, Germany, 1986.
(31) Least-squares: function minimized $\Sigma w(|F_o| - |F_c|)^2$ where $w = 4F_o^2/\sigma^2(F_o^2)$; $\sigma^2(F_o^2) = [S^2(C + R^2B) + (pF_o^2)^2]/L_p^2$; S = scan rate, C = total integrated peak count, R = ratio of scan time to background counting time, B = total background count, L_p = Lorentz–polarization factor, p = p factor.
(32) Cromer, D. T.; Waber, J. T. In *International Tables for X-ray Crystallography*; Ibers, J. A., Hamilton, W. C., Eds.; The Kynoch Press: Birmingham, England, 1974; Vol. IV, Table 2.2 A.
(33) Ibers, J. A.; Hamilton, W. C. *Acta Crystallogr.* **1964**, *17*, 781.
(34) Cromer, D. T. In *International Tables for X-ray Crystallography*; Ibers, J. A., Hamilton, W. C., Eds.; The Kynoch Press: Birmingham, England, 1974; Vol. IV, Table 2.3.1.
(35) Swepston, P. N. *TEXSAN, Version 4.0. The TEXRAY Structure Analysis Program Package*; Molecular Structure Corp.: The Woodlands, TX, 1987.
(36) Deeming, A. J.; Ettore, R.; Johnson, B. F. G.; Lewis, J. *J. Chem. Soc. A* **1971**, 1797.

Scheme 2

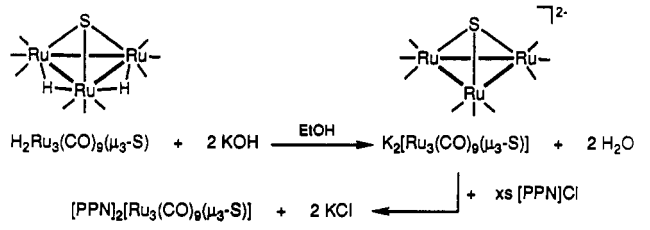

Brown and co-workers recently prepared $[PPN]_2[Ru_3(CO)_9(\mu_3\text{-}S)]$,[11] in high yield by the deprotonation of the hydrido cluster $H_2Ru_3(CO)_9(\mu_3\text{-}S)$. A solid product was obtained by metathesis with [PPN]Cl (Scheme 2). In our hands, the literature procedure for $[PPN]_2[Ru_3(CO)_9(\mu_3\text{-}S)]$ failed to yield a clean crystalline product; however, a modified procedure, presented in the Experimental Section, yielded bright yellow crystals of high purity, but the yield, 30%, was much lower than that in the previous report, 82%.[11]

Synthesis and Characterization of the Mixed-Metal Sulfido Clusters $HRu_3(CO)_9(\mu_4\text{-}S)M(CO)_3(NCCH_3)_2$ (M = Mn, Re). The reaction of the μ_3-sulfido cluster $[Ru_3(CO)_9(\mu_3\text{-}S)]^{2-}$ with 1 equiv of the labile cation $[Mn(CO)_3(NCCH_3)_3]^+$ yields the metal-capped sulfido cluster $HRu_3(CO)_9(\mu_4\text{-}S)Mn(CO)_3(NCCH_3)_2$ (eq 2). In this reaction two acetonitrile ligands are retained on the manganese center.

(2)

Two ^1H NMR signals are observed for $HRu_3(CO)_9(\mu_4\text{-}S)Mn(CO)_3(NCCH_3)_2$: one at 2.32 ppm for the methyl protons of the coordinated acetonitrile ligands and the other at −18.72 ppm for the bridging hydride coordinated to the ruthenium–metal framework. The very similar cluster $HRu_3(CO)_9(\mu_4\text{-}S)Ru(CO)_3(\eta^2\text{-}CH_2CMe_2NHCNHBu^t)$[37] has a hydride resonance at −18.69 ppm. For reference, the cluster $H_2Ru_3(CO)_9(\mu_3\text{-}S)$ has a hydride resonance at −18.95 ppm (lit.[28] value −18.98 ppm) relative to TMS. A very small peak is also observed in the ^1H NMR spectrum of $HRu_3(CO)_9(\mu_4\text{-}S)Mn(CO)_3(NCCH_3)_2$ at 2.38 ppm, which varies in intensity from sample to sample and may indicate residual $[Mn(CO)_3(NCCH_3)_3][PF_6]$.

A negative-ion liquid secondary ion (FABMS) mass spectrum of $HRu_3(CO)_9(\mu_4\text{-}S)Mn(CO)_3(NCCH_3)_2$ (Figure 2) contained the most abundant and highest mass feature at m/z 811, which corresponds to $[HRu_3(CO)_9(\mu_4\text{-}S)Mn(CO)_3(NCCH_3)_2]^-$.

The fragmentation pattern in the spectrum of $HRu_3(CO)_9(\mu_4\text{-}S)Mn(CO)_3(NCCH_3)_2$ is typical of those observed for carbonyl compounds.[38] Loss of a carbonyl ligand is indicated by a change of 28 in m/z, and a similar loss of an acetonitrile ligand is shown by a change of 41 in m/z. The spectrum has abundant ions characteristic of ligand loss. The fragmentation pattern for this compound indicates an ion due to the loss of one acetonitrile (m/z 770) and then further fragmentation ions. The most abundant ions result from loss of at least nine consecutive carbonyl ligands (m/z 742, 714, 686, 658, 630, 602, 574, 546, 518), and

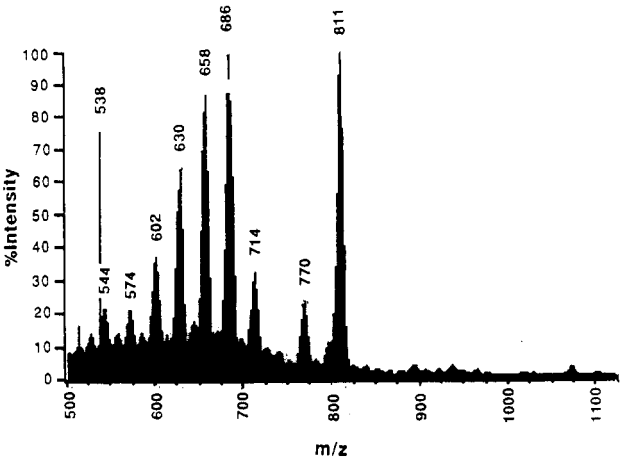

Figure 2. Negative-ion FABMS spectrum of $HRu_3(CO)_9(\mu_4\text{-}S)Mn(CO)_3(NCCH_3)_2$ in *m*-NBA. Major peaks are labeled with the observed m/z value.

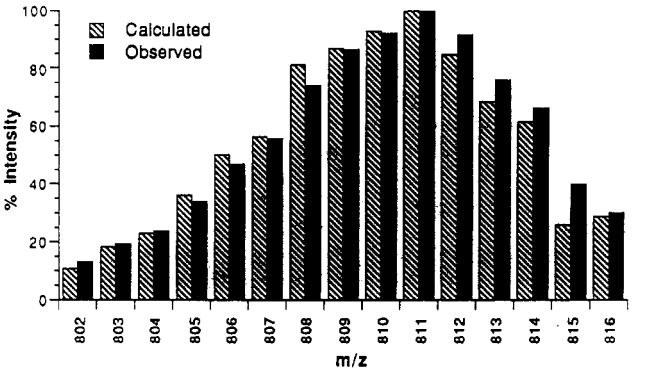

Figure 3. Observed (solid bar) isotope distribution in the vicinity of m/z 811 in the FABMS spectrum for Cs^+ bombardment of $HRu_3(CO)_9(\mu_4\text{-}S)Mn(CO)_3(NCCH_3)_2$. Dashed bars correspond to the calculated isotopomers of $[HRu_3(CO)_9(\mu_4\text{-}S)Mn(CO)_3(NCCH_3)_2]^-$.

the low-abundance ions result from loss of the second acetonitrile ligand (m/z 729), followed by loss of two carbonyl ligands (m/z 673) and then loss of at least five consecutive carbonyl ligands (m/z 645, 617, 589, 561, 533).

For the seven isotopes of ruthenium, the four isotopes of sulfur, the two isotopes each of carbon, oxygen, and nitrogen, and the one isotope each of hydrogen and manganese, a wide distribution of peaks (or envelope) would be expected for each ionic species. The isotopic distribution of the envelope surrounding the molecular ion at m/z 811 matches that expected for $[HRu_3(CO)_9(\mu_4\text{-}S)Mn(CO)_3(NCCH_3)_2]^-$ (Figure 3). The low value of $R = 0.062$ indicates good agreement between the calculated mass distribution for $[HRu_3(CO)_9(\mu_4\text{-}S)Mn(CO)_3(NCCH_3)_2]^-$ and the observed mass spectrum. Thus, the mass spectral data are consistent with the X-ray structural data for the cluster $HRu_3(CO)_9(\mu_4\text{-}S)Mn(CO)_3(NCCH_3)_2$, discussed below.

A second sample in which an excess (2 equiv) of $[Mn(CO)_3(NCCH_3)_2][PF_6]$ was used in the synthesis gave a FABMS spectrum with an additional peak at m/z 894, the highest mass ion, but in low abundance (see supplementary material). Again, the isotopic distribution of the envelope surrounding the molecular ion at m/z 811 matches that expected for $[HRu_3(CO)_9(\mu_4\text{-}S)Mn(CO)_3(NCCH_3)_2]^-$ with $R = 0.057$. The isotopic distribution of the envelope surrounding the highest mass ion at m/z 894 matches that expected for $[Mn_2Ru_3(CO)_{16}(S)]^-$, with $R = 0.135$.

The presence of the m/z 894 peak in the FABMS provides evidence for some loss of the acetonitrile ligands and formation of a higher nuclearity five-metal sulfido cluster, presumably Mn_2-

(37) Bodensieck, U.; Stoeckli-Evans, H.; Suss-Fink, G. *J. Chem. Soc., Chem. Commun.* **1990**, *182*, 267.
(38) Naylor, S.; Vargas, M. D. *J. Organomet. Chem.* **1990**, *386*, 275.

$Ru_3(CO)_{16}(\mu_4\text{-S})$. Cluster valence electron counting rules[39] indicate that this 74-electron cluster should have a geometry of a square pyramid of metals with a μ_4-S ligand on the square base, similar to the geometry observed for the mixed-metal oxo cluster $[Fe_2Ru_3(CO)_{14}(\mu_4\text{-O})]^{2-}$ isolated in our laboratory.[40] The cluster $Mn_2Ru_3(CO)_{16}(\mu_4\text{-S})$, however, was not isolated.

In contrast to the chemistry of the ruthenium cluster $[Ru_3(CO)_9(\mu_3\text{-S})]^{2-}$ described here, the butterfly sulfido cluster $[Fe_3Mn(CO)_{12}(\mu_4\text{-S})]^-$ forms when 1 equiv of $[Mn(CO)_3(NCCH_3)_2]^+$ reacts with $[Fe_3(CO)_9(\mu_3\text{-S})]^{2-}$ in acetone (eq 3).[7] This butterfly

(3)

cluster $[Fe_3Mn(CO)_{12}(\mu_4\text{-S})]^-$ forms quickly and easily, in high yield, and a single-crystal X-ray structure determination confirmed the butterfly geometry.

The reaction of $[Ru_3(CO)_9(\mu_3\text{-S})]^{2-}$ with $[Re(CO)_3(NCCH_3)_3]^+$ proceeded extremely slowly in dichloromethane and only slightly faster in acetone. However, the reaction in acetone was allowed to progress over a prolonged time, and after 4 days of stirring, the pseudotetrahedral sulfido cluster $HRu_3(CO)_9(\mu_4\text{-S})Re(CO)_3(NCCH_3)_2$ was isolated (eq 4). The infrared spectrum of the

(4)

mixed-metal rhenium and ruthenium sulfido cluster resembles that for $HRu_3(CO)_9(\mu_4\text{-S})Mn(CO)_3(NCCH_3)_2$, indicating an analogous formulation, $HRu_3(CO)_9(\mu_4\text{-S})Re(CO)_3(NCCH_3)_2$. The IR spectra of these two clusters also match well with the spectrum of the previously reported diaminocarbene cluster $HRu_3(CO)_9(\mu_4\text{-S})Ru(CO)_3(\eta^2\text{-}CH_2CMe_2NHCNHBu^t)$[37] (Table 1).

The slow reaction of $[Re(CO)_3(NCCH_3)_3]^+$ compared to that of $[Mn(CO)_3(NCCH_3)_3]^+$ was also observed in their reactions with the nucleophile $[Fe_3(CO)_9(\mu_3\text{-S})]^{2-}$.[7] The reaction with $[Re(CO)_3(NCCH_3)_2]^+$ proceeded so slowly that it was not pursued.

Further evidence for the formulation $HRu_3(CO)_9(\mu_4\text{-S})Re(CO)_3(NCCH_3)_2$ was provided by FABMS mass spectrometry (see supplementary material), which indicates a molecular ion cluster $[M]^-$ at m/z 941 corresponding to $[HRu_3(CO)_9(\mu_4\text{-S})Re(CO)_3(NCCH_3)_2]^-$ as the highest mass ion. The isotopic analysis yielded $R = 0.105$. Thus, the mass spectral data are consistent with the assignment of the cluster as $HRu_3(CO)_9(\mu_4\text{-S})Re(CO)_3(NCCH_3)_2$ based on infrared spectroscopic evidence.

Structure of $HRu_3(CO)_9(\mu_4\text{-S})Mn(CO)_3(NCCH_3)_2$. The ORTEP[41] drawing of the cluster $HRu_3(CO)_9(\mu_4\text{-S})Mn(CO)_3(NCCH_3)_2$ with selected atom labels is shown in Figure 4. Details of the structure, including positional parameters and selected bond distances and angles, are summarized in Tables 3 and 4.

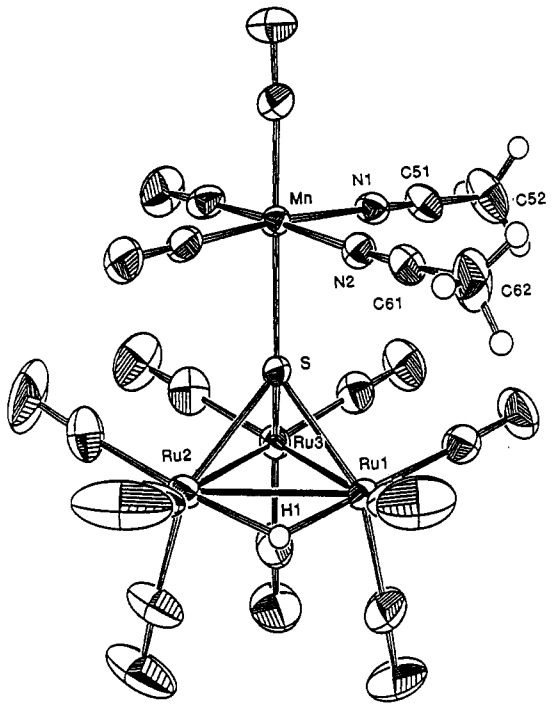

Figure 4. ORTEP drawing of $HRu_3(CO)_9(\mu_4\text{-S})Mn(CO)_3(NCCH_3)_2$. Thermal ellipsoids are drawn at a 50% probability level.

The cluster $HRu_3(CO)_9(\mu_4\text{-S})Mn(CO)_3(NCCH_3)_2$ consists of a nearly equalateral triangle of ruthenium atoms capped by a μ_3-sulfido ligand. The sulfido ligand is also coordinated to a "pendant" manganese atom, making the overall coordination of the sulfur atom μ_4, with pseudotetrahedral coordination. Alternately, the cluster can be viewed as a ruthenium triangle capped with a pendant $\mu_3\text{-}SMn(CO)_3(NCCH_3)_2$ group, represented by the formula $HRu_3(CO)_9(\mu_3\text{-}SMn(CO)_3(NCCH_3)_2)$. No metal–metal bonds are made in the formation of $HRu_3(CO)_9(\mu_3\text{-}SMn(CO)_3(NCCH_3)_2)$, unlike the formation of the butterfly sulfido cluster $[Fe_3Mn(CO)_{12}(\mu_4\text{-S})]^-$ (Figure 5).[7]

The quadruply bridging sulfido ligand in $HRu_3(CO)_9(\mu_4\text{-S})Mn(CO)_3(NCCH_3)_2$ serves as a six-electron donor, and the metal atoms in the cluster attain 18-electron configurations. With respect to the Ru_3 skeleton, the S atom functions as a five-electron donor, making the electron count for this part of the molecule 48, as expected for a triangular cluster. The $Mn(CO)_3(NCCH_3)_2$ moiety receives one electron from the sulfur atom to complete its valence electron count of 18. The total electron count for this cluster is 66.

The bonding around the sulfido ligand can be viewed as distorted tetrahedral, where the Ru–S–Ru angles within the Ru_3 core are acute (Ru1–S–Ru2 = 75.11(5)°, Ru2–S–Ru3 = 72.88(5)°, Ru1–S–Ru3 = 73.28(5)°) and the Ru–S–Mn angles are fairly large (Ru1–S–Mn = 137.08(7)°, Ru2–S–Mn = 134.80(7)°, Ru3–S–Mn = 136.48(7)°). This geometry results because the metal–metal-bonded Ru_3 triangle restricts the angles around the sulfur atom. These metal–sulfido–metal angles strengthen the description of the cluster as $HRu_3(CO)_9(\mu_3\text{-}SMn(CO)_3(NCCH_3)_2)$. The distances from the sulfur atom to the four metals are roughly equal (Ru1–S = 2.338(2) Å, Ru2–S = 2.335(2) Å, Ru3–S = 2.328(2) Å, Mn–S = 2.365(2) Å) although the manganese atom is slightly further away. The manganese–sulfur distance in this cluster is considerably longer than the distance of 2.274(1) Å observed in the mixed-metal butterfly sulfido cluster $[Fe_3Mn(CO)_{12}(\mu_4\text{-S})]^-$ (Figure 5).[7]

In the cluster $HRu_3(CO)_9(\mu_3\text{-}SMn(CO)_3(NCCH_3)_2)$, three terminal carbonyl ligands coordinate to each ruthenium atom.

(39) Lauher, J. W. *J. Am. Chem. Soc.* **1978**, *100*, 5305.
(40) Schauer, C. K.; Voss, E. J.; Sabat, M.; Shriver, D. F. *J. Am. Chem. Soc.* **1989**, *111*, 7662.
(41) Johnson, C. K. ORTEP-II: A FORTRAN Thermal-Ellipsoid Plot Program. Report ORNL-5138; Oak Ridge National Laboratory: Oak Ridge, TN, 1976.

Table 3. Positional and Thermal Parameters and Their Estimated Standard Deviations for $HRu_3(CO)_9(\mu_4\text{-}S)Mn(CO)_3(NCCH_3)_2$

atom	x	y	z	B(eq),[a] Å²
Ru1	0.68852(3)	0.10832(5)	0.46055(3)	2.27(2)
Ru2	0.77884(3)	0.06431(5)	0.33332(3)	2.14(2)
Ru3	0.64327(3)	-0.11260(6)	0.35095(3)	2.44(2)
Mn	0.85239(5)	-0.2795(1)	0.50351(5)	1.87(3)
S	0.76494(9)	-0.1035(2)	0.43352(8)	1.90(5)
O11	0.5681(5)	0.3502(9)	0.4011(4)	9.2(5)
O12	0.5855(3)	-0.0337(7)	0.5753(3)	5.5(3)
O13	0.8039(4)	0.2897(6)	0.5746(4)	6.9(4)
O21	0.6915(4)	0.2702(9)	0.2123(4)	8.0(4)
O22	0.8573(5)	-0.1510(9)	0.2301(4)	8.0(4)
O23	0.9411(4)	0.2291(7)	0.3730(5)	8.8(4)
O31	0.5145(4)	0.0688(9)	0.2526(4)	7.5(4)
O32	0.5244(3)	-0.2947(6)	0.4343(3)	4.8(3)
O33	0.6782(4)	-0.3524(7)	0.2349(3)	5.8(3)
O41	0.9605(3)	-0.5058(5)	0.5884(3)	3.8(2)
O42	0.8195(3)	-0.4862(5)	0.3719(3)	4.3(2)
O43	0.9914(3)	-0.1496(5)	0.4331(3)	3.7(2)
N1	0.7518(3)	-0.3511(5)	0.5479(3)	2.3(2)
N2	0.8678(3)	-0.1320(5)	0.5907(3)	2.2 (2)
C11	0.6143(5)	0.261(1)	0.4259(5)	5.0(4)
C12	0.6244(4)	0.0222(8)	0.5323(4)	3.5(3)
C13	0.7615(5)	0.2210(8)	0.5310(5)	4.1(3)
C21	0.7255(5)	0.193(1)	0.2564(5)	4.8(4)
C22	0.8254(5)	-0.068(1)	0.2667(4)	4.4(4)
C23	0.8788(5)	0.1692(8)	0.3609(5)	4.8(4)
C31	0.5624(5)	-0.002(1)	0.2885(4)	4.5(4)
C32	0.5701(4)	-0.2268(8)	0.4030(4)	3.4(3)
C33	0.6640(4)	-0.264(1)	0.2785(4)	3.6(3)
C41	0.9184(4)	-0.4178(6)	0.5576(4)	2.5(2)
C42	0.8326(4)	-0.4073(6)	0.4234(4)	2.7(3)
C43	0.9384(4)	-0.2005(7)	0.4614(4)	2.5(2)
C51	0.6935(4)	-0.3921(7)	0.5699(3)	2.7(3)
C52	0.6194(5)	-0.445(1)	0.5985(4)	4.5(4)
C61	0.8797(4)	-0.0517(7)	0.6403(4)	2.9(3)
C62	0.8978(6)	0.049(1)	0.7069(4)	5.0(4)
H1	0.7456	0.1852	0.4033	2.7
H52A	0.5854	-0.3600	0.6062	5.7
H52B	0.5908	-0.5097	0.5612	5.7
H52C	0.6326	-0.4967	0.6449	5.7
H62A	0.8942	-0.004	0.7528	6.1
H62B	0.9478	0.0989	0.7056	6.1
H62C	0.8545	0.1299	0.7024	6.1

[a] Anisotropically refined atoms are given in the form of the isotropic equivalent thermal parameter defined as $(4/3)[a^2B(1,1) + b^2B(2,2) + c^2B(3,3) + ab(\cos\gamma)B(1,2) + ac(\cos\beta)(B(1,3) + bc(\cos\alpha)B(2,3)]$.

Table 4. Selected Intramolecular Distances and Bond Angles for $HRu_3(CO)_9(\mu_4\text{-}S)Mn(CO)_3(NCCH_3)_2$[a]

	Distances (Å)		
Ru1–Ru2	2.848(1)	Ru2–H1	1.74
Ru1–Ru3	2.784(1)	Ru3–S	2.328(2)
Ru1–S	2.338(2)	Mn–S	2.365(2)
Ru1–H1	1.604	Mn–N1	2.010(5)
Ru2–Ru3	2.770(1)	Mn–N2	2.006(5)
Ru2–S	2.335(2)		
	Angles (deg)		
Ru2–Ru1–Ru3	58.90(2)	Ru3–Ru2–S	53.43(4)
Ru2–Ru1–S	52.40(4)	Ru3–Ru2–H1	87.01
Ru2–Ru1–H1	34.02	S–Ru2–H1	78.29
Ru3–Ru1–S	53.19(4)	Ru1–Ru3–Ru2	61.71(2)
Ru3–Ru1–H1	89.68	Ru1–Ru3–S	53.53(4)
S–Ru1–H1	81.22	Ru2–Ru3–S	53.68(4)
Ru1–Ru2–Ru3	59.40(2)	Ru1–S–Ru2	75.11(5)
Ru1–Ru2–S	52.49(4)	Ru1–S–Ru3	73.28(5)
Ru1–Ru2–H1	30.57	Ru1–S–Mn	137.08(7)
Ru2–S–Mn	134.80(7)	Ru2–S–Ru3	72.88(5)
Ru3–S–Mn	136.48(7)		

[a] Estimated standard deviations in the least significant figure are given in parentheses.

The manganese atom is bonded to five terminal groups (three carbonyl ligands and two acetonitrile ligands) and is octahedrally coordinated. Two manganese-coordinated carbonyl ligands are equatorial and one is axial; the acetonitrile ligands on the manganese center are equatorial and *cis* to each other. The hydride ligand in $HRu_3(CO)_9(\mu_3\text{-}SMn(CO)_3(NCCH_3)_2)$, located in the X-ray structure determination, bridges between Ru1 and Ru2 on the ruthenium framework. The angles Ru2–Ru1–H1 = 34.02° and Ru1–Ru2–H1 = 30.57° are normal for a bridging hydride. The bond distances Ru1–H1 = 1.604 Å and Ru2–H1 = 1.764 Å are similar to distances observed in other ruthenium clusters containing a bridging hydride ligand; e.g., for $(\mu\text{-}H)_2Ru_3(CO)_9(\mu_3\text{-}S)$ Ru1–H1 = 1.67(5) Å, Ru2–H1 = 1.59(5) Å, Ru2–H2 = 1.69(4) Å, and Ru3–H2 = 1.75(5) Å.[26] Ruthenium–hydride distances for $(\mu\text{-}H)_2Ru_3(CO)_8(\mu\text{-}Cl)(SnCl_3)$ are: Ru1–H1 = 1.64(6) Å, Ru2–H1 = 1.81(6) Å, Ru2–H2 = 1.77(6) Å, and Ru3–H2 = 1.76(6) Å.[26] Although a bridging hydride exists on the similar cluster $HRu_3(CO)_9(\mu_4\text{-}S)Ru(CO)_3(\eta^2\text{-}CH_2CMe_2NHCNHBu^t)$,[37] the hydride ligand was not located in that X-ray structure determination. Sulfido clusters analogous to $HRu_3(CO)_9(\mu_4\text{-}S)Mn(CO)_3(NCCH_3)_2$ and $HRu_3(CO)_9(\mu_4\text{-}S)Re(CO)_3(NCCH_3)_2$ are known.[12,13,37,42-44]

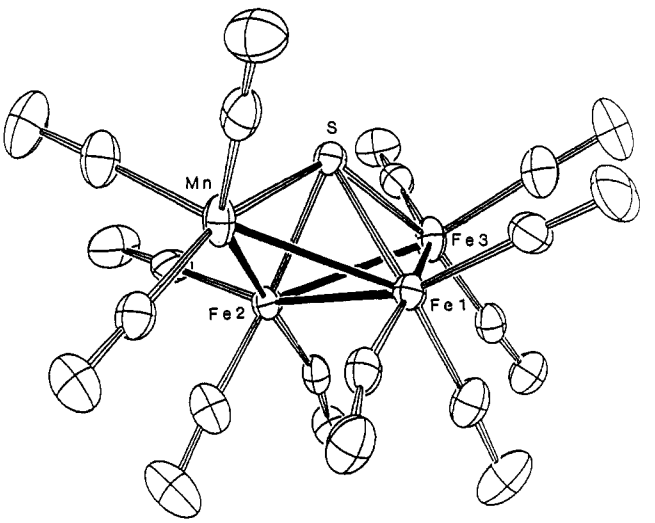

Figure 5. ORTEP drawing of $[Fe_3Mn(CO)_{12}(\mu_4\text{-}S)]^-$. Thermal ellipsoids are drawn at a 50% probability level.

Reaction of $[Ru_3(CO)_9(\mu_3\text{-}S)]^{2-}$ with $[M(CO)_5]^+$ To Form the Mixed-Metal Sulfido Clusters $HRu_3(CO)_9(\mu_4\text{-}S)M(CO)_5$ (M = Mn, Re). In reaction chemistry similar to that employed to form the pendant clusters $HRu_3(CO)_9(\mu_4\text{-}S)Mn(CO)_3(NCCH_3)_2$ and $HRu_3(CO)_9(\mu_4\text{-}S)Re(CO)_3(NCCH_3)_2$, $[Ru_3(CO)_9(\mu_3\text{-}S)]^{2-}$ was allowed to react with 1 equiv of the electrophilic cluster building reagent $[Mn(CO)_5][SO_3CF_3]$ or $[Re(CO)_5][SO_3CF_3]$[25] with the idea of forming clusters containing a pendant $M(CO)_5$ unit, (eq 5). Solution infrared spectra of the products (Table 1) indicate

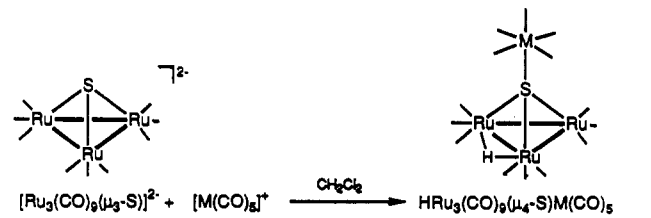

(5)

the presence of the mixed-metal sulfido clusters $HRu_3(CO)_9(\mu_4\text{-}S)Mn(CO)_5$ and $HRu_3(CO)_9(\mu_4\text{-}S)Re(CO)_5$, but crystalline products could not be isolated. FABMS data suggest either that

(42) Hoefler, M.; Tebbe, K.; Veit, H.; Weiler, N. E. *J. Am. Chem. Soc.* **1983**, *105*, 6338.
(43) Adams, R. D.; Mannig, D.; Segmuller, B. E. *Organometallics* **1983**, *2*, 149.
(44) Adams, R. D.; Horvath, I. T.; Wang, S. *Inorg. Chem.* **1985**, *24*, 1728.

Scheme 3

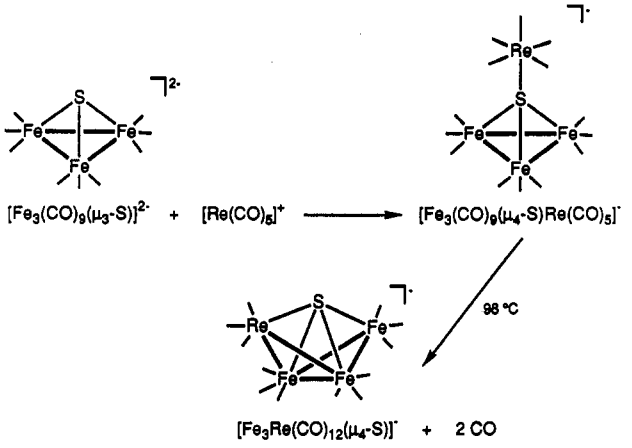

the isolated oils from these reactions are mixtures of products or that these clusters readily lose the "pendant" metal under the conditions used to obtain mass spectra.

The acetonitrile-substituted cluster $HRu_3(CO)_9(\mu_4\text{-}S)Mn(CO)_3(NCCH_3)_2$ was allowed to stir in acetone solution under a carbon monoxide atmosphere for several days. The resulting yellow solution has an infrared spectrum similar to that for $HRu_3(CO)_9(\mu_4\text{-}S)Mn(CO)_5$ obtained by direct reaction of $[Ru_3(CO)_9(\mu_3\text{-}S)]^{2-}$ with $[Mn(CO)_5]^+$ (Table 1). This experiment provides further evidence for the existence of the clusters $HRu_3(CO)_9(\mu_4\text{-}S)Mn(CO)_5$ and $HRu_3(CO)_9(\mu_4\text{-}S)Re(CO)_5$.

In similar chemistry in our research group, Schauer reacted the iron sulfido cluster $[Fe_3(CO)_9(\mu_3\text{-}S)]^{2-}$ with $[Re(CO)_5]^+$ to form the pendant rhenium pentacarbonyl sulfido cluster $[Fe_3(CO)_9(\mu_4\text{-}S)Re(CO)_5]^-$.[45] This pendant sulfido cluster was then employed in the synthesis of the butterfly cluster $[Fe_3Re(CO)_{12}(\mu_4\text{-}S)]^-$, the rhenium analog of the manganese–iron butterfly cluster $[Fe_3Mn(CO)_{12}(\mu_4\text{-}S)]^-$. Upon refluxing in 1,2- dichloroethane, $[Fe_3(CO)_9(\mu_4\text{-}S)Re(CO)_5]^-$ loses two carbonyl ligands and rearranges into the butterfly cluster $[Fe_3Re(CO)_{12}(\mu_4\text{-}S)]^-$ (Scheme 3).[7] The manganese analog $[Fe_3(CO)_9(\mu_4\text{-}S)Mn(CO)_5]^-$ was also synthesized by Schauer and, upon heating, was shown to rearrange into the butterfly sulfido cluster $[Fe_3Mn(CO)_{12}(\mu_4\text{-}S)]^-$.[45]

Takacs and Marko also observed capping $M(CO)_5$ units from the reactions of the anionic sulfido clusters $[HFe_3(CO)_9(\mu_3\text{-}S)]^-$ and $[Fe_3(CO)_9(\mu_3\text{-}S)]^{2-}$ with $M(CO)_5(THF)$ (M = Cr, W).[13] The resulting compounds, $[Fe_3(CO)_9(\mu_4\text{-}S)M(CO)_5]^{2-}$ and $[HFe_3(CO)_9(\mu_4\text{-}S)M(CO)_5]^-$ (M = Cr, W) were isolated and characterized by C, H, and N analyses and infrared spectroscopy. They found that coordinating solvents such as acetonitrile cleaved the M–S bond in $[HFe_3(CO)_9(\mu_4\text{-}S)M(CO)_5]^-$ (M = Cr, W) within 1 h. Cleavage of the dianionic clusters $[Fe_3(CO)_9(\mu_4\text{-}S)M(CO)_5]^{2-}$ (M = Cr, W) proceeded slowly over the course of 1 week. The instability of the monoanionic iron clusters is in agreement with our inability to isolate the neutral $M(CO)_5$-capped clusters $HRu_3(CO)_9(\mu_4\text{-}S)M(CO)_5$ (M = Mn, Re). FABMS spectra of these ruthenium clusters show large-abundance peaks for $[HRu_3(CO)_9(\mu_3\text{-}S)]^-$, indicating similar cleavage of the M–S bond.

One major difference between the chemistry of $[Ru_3(CO)_9(\mu_3\text{-}S)]^{2-}$ and the iron analog $[Fe_3(CO)_9(\mu_3\text{-}S)]^{2-}$ is the ease of protonation of the ruthenium framework in the cluster-building reactions. The isolated mixed-metal ruthenium sulfido clusters $HRu_3(CO)_9(\mu_4\text{-}S)Mn(CO)_3(NCCH_3)_2$ and $HRu_3(CO)_9(\mu_4\text{-}S)Re(CO)_3(NCCH_3)_2$ are neutral and contain a proton on their ruthenium framework, whereas the mixed-metal iron sulfido clusters $[Fe_3(CO)_9(\mu_4\text{-}S)Re(CO)_5]^-$, $[Fe_3Mn(CO)_{12}(\mu_4\text{-}S)]^-$, and $[Fe_3Re(CO)_{12}(\mu_4\text{-}S)]^-$ could be isolated as anions without protonation. The greater basicity and reactivity of a ruthenium cluster compared to the iron analog was also observed in the chemistry of the oxo cluster $[Ru_3(CO)_9(\mu_3\text{-}O)]^{2-}$ discussed elsewhere.[46]

Although carefully dried solvents were employed in oven-baked glassware, the proton source for the ruthenium sulfido clusters is believed to be a small amount of moisture in the solvent or on the glassware. Initial reactions were performed in acetone, a solvent that is difficult to completely dry. However, even when carefully dried dichloromethane was employed as the solvent, protonation took place.

In the present research the sulfur atom of $[Ru_3(CO)_9(\mu_3\text{-}S)]^{2-}$ serves as a nucleophile to lightly coordinated organometallics, with no metal–metal bonds formed. In contrast, Brown and coworkers found that $[Ru_3(CO)_9(\mu_3\text{-}S)]^{2-}$ combines with coinage metal phosphines through ruthenium–coinage metal bonds, with no metal–sulfur bond formation (see Scheme 1).[11] Similarly, mixed-four- and five-metal sulfido clusters $HAuRu_3(CO)_8(PPh_3)L(\mu_3\text{-}S)$ and $Au_2Ru_3(CO)_8(PPh_3)_2L(\mu_3\text{-}S)$ (L = CO, PPh_3)[47,48] consist of two fused triangles with a μ_3-sulfido ligand on the exterior of the framework. The reactivity of Cu, Ag, or Au metal fragments at metal–metal bonds may be rationalized after the fact by the isolobal relation between the M(I) coinage metals and the proton which has a high affinity for low-oxidation-state metals.[49]

Conclusions

The ruthenium sulfido clusters $H_2Ru_3(CO)_9(\mu_3\text{-}S)$ and $[Ru_3(CO)_9(\mu_3\text{-}S)]^{2-}$ are easily prepared in high yields. The anionic cluster $[Ru_3(CO)_9(\mu_3\text{-}S)]^{2-}$ is a useful precursor to higher nuclearity mixed-metal sulfido clusters and displays interesting diversity in its reactions with metal electrophiles. With coinage metal phosphines it has been shown to form metal–metal bonds. In contrast, $[Ru_3(CO)_9(\mu_3\text{-}S)]^{2-}$ reacts through the sulfur atom with $[M(CO)_3(NCCH_3)_3]^+$ and $[M(CO)_5]^+$ (M = Mn, Re), yielding the pendant clusters $HRu_3(CO)_9(\mu_4\text{-}S)Mn(CO)_3(NCCH_3)_2$, $HRu_3(CO)_9(\mu_4\text{-}S)Re(CO)_3(NCCH_3)_2$, $HRu_3(CO)_9(\mu_4\text{-}S)Mn(CO)_5$, and $HRu_3(CO)_9(\mu_4\text{-}S)Re(CO)_5$. Part of this difference may be due to the formation of Ru–H bonds, which suppress the nucleophilicity of the Ru_3 cluster.

A different type of reaction is observed with $[Fe_3(CO)_9(\mu_3\text{-}S)]^{2-}$, which forms butterfly products $[Fe_3Mn(CO)_{12}(\mu_4\text{-}S)]^-$ and $[Fe_3Re(CO)_{12}(\mu_4\text{-}S)]^-$.

Acknowledgment. We are grateful for support of this work by Department of Energy Grant No. DE-FG02-86-ER13640. We wish to thank Dr. H. Hung for mass spectral analysis.

Supplementary Material Available: Tables of crystal structure data, positional parameters, anisotropic thermal parameters, and bond distances and angles, an ORTEP diagram showing the atom numbering scheme for $HRu_3(CO)_9(\mu_4\text{-}S)Re(CO)_3(NCCH_3)_2$, figures of FABMS spectra and isotope distributions, and tables of FABMS fragmentation (27 pages). Ordering information is given on any current masthead page.

(45) Schauer, C. K. Personal communication.

(46) Voss, E. J.; Sabat, M.; Shriver, D. F. Manuscript in preparation.
(47) Farrugia, L. J.; Freeman, M. J.; Green, M.; Orpen, A. G.; Stone, F. G. A.; Salter, I. D. *J. Organomet. Chem.* **1983**, *249*, 273.
(48) Bruce, M. I.; Shawkataly, O. B.; Nicholson, B. K. *J. Organomet. Chem.* **1985**, *286*, 427.
(49) Salter, I. D. *Adv. Organomet. Chem.* **1989**, *29*, 249.